Neuron, Volume *109*

Supplemental information

Regional, Layer, and Cell-Type-Specific Connectivity of the Mouse Default Mode Network

Jennifer D. Whitesell, Adam Liska, Ludovico Coletta, Karla E. Hirokawa, Phillip Bohn, Ali Williford, Peter A. Groblewski, Nile Graddis, Leonard Kuan, Joseph E. Knox, Anh Ho, Wayne Wakeman, Philip R. Nicovich, Thuc Nghi Nguyen, Cindy T.J. van Velthoven, Emma Garren, Olivia Fong, Maitham Naeemi, Alex M. Henry, Nick Dee, Kimberly A. Smith, Boaz Levi, David Feng, Lydia Ng, Bosiljka Tasic, Hongkui Zeng, Stefan Mihalas, Alessandro Gozzi, and Julie A. Harris

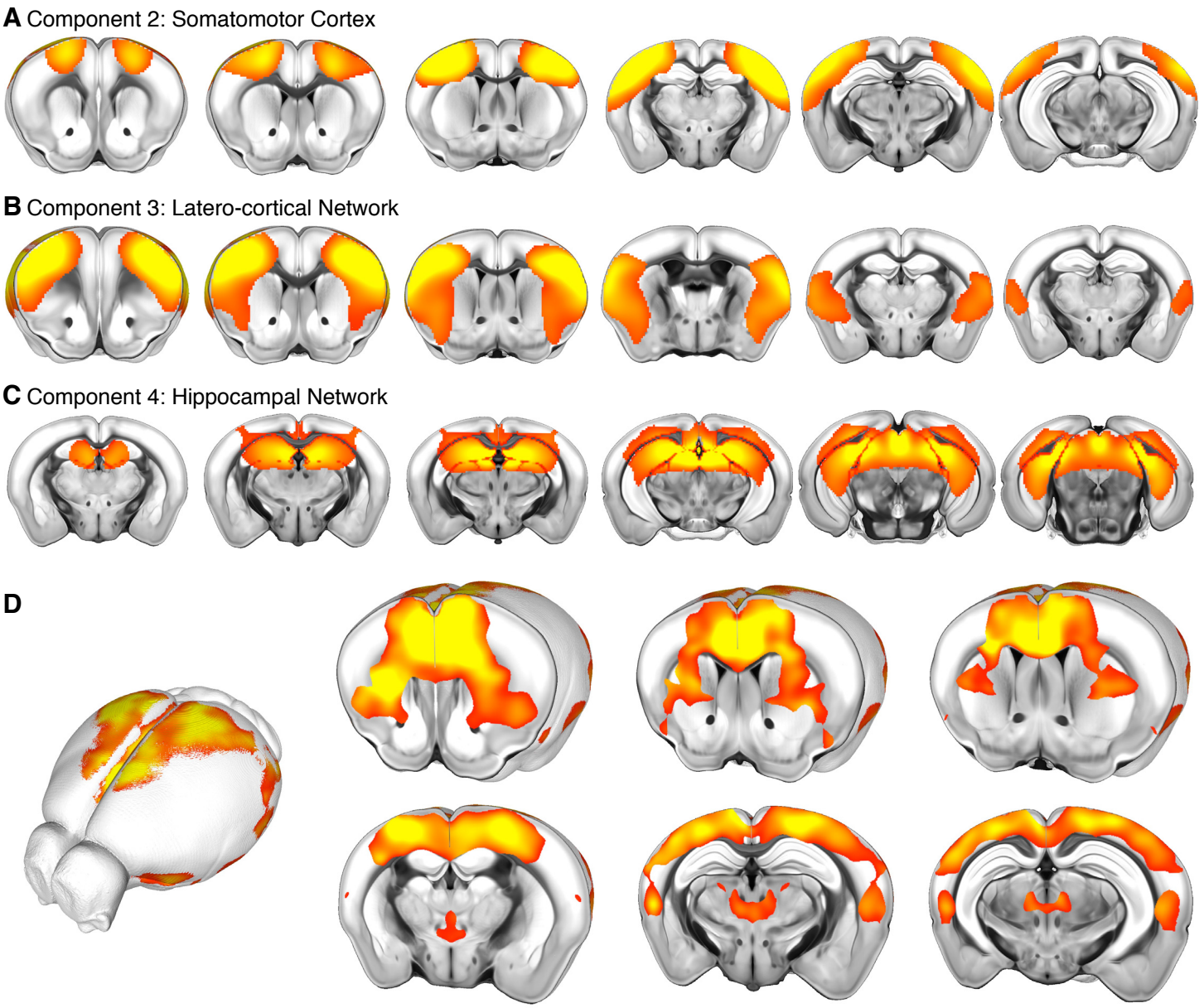

Figure S1 related to Figure 1. Overlap of functional networks with major brain divisions
(A-C) Additional components identified with indepenent component analysis (ICA) on resting state fMRI data. (D) An alternative DMN component generated with a seed pixel in ACA resembles the ICA map in **Figure 1B,C**. (E-G) Pie charts showing the composition of each component in terms of major brain divisions. Abbreviations: TH: thalamus, MB: midbrain, OLF: olfactory areas, CTXsp: cortical subplate, HPF: hippocampal formation, STR: striatum, PAL: pallidum.

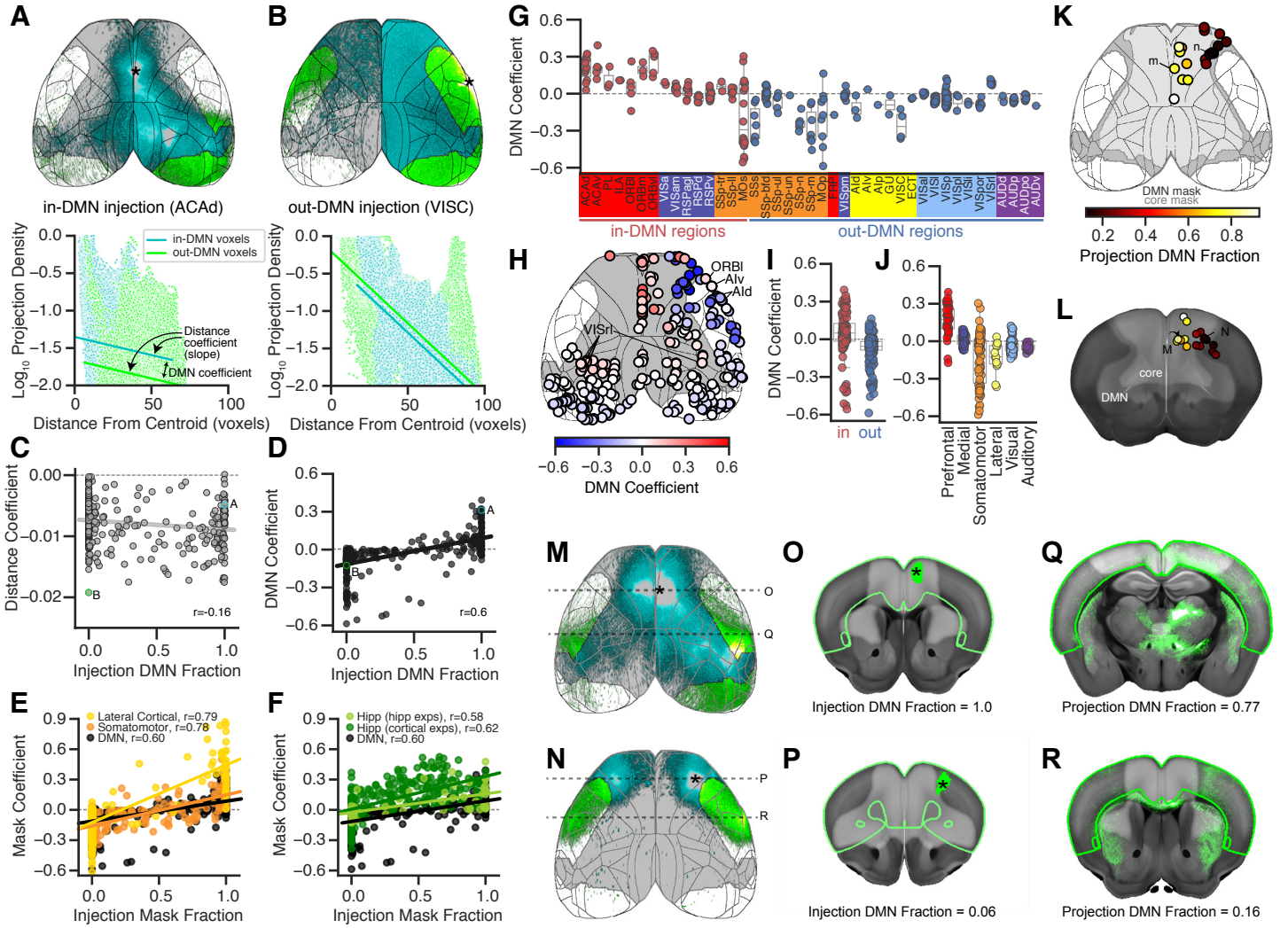

Figure S2 related to Figure 2. Preferential DMN connectivity independent of distance and region boundaries
(A,B) Cortical projections (top) and projection density per isocortex voxel (bottom) plotted for in-DMN voxels (cyan) and out-DMN voxels (green) in one in-DMN (A) and one out-DMN (B) experiment. Lines on bottom plots show the model fit for in-DMN voxels (cyan) and out-DMN voxels (green). The magnitude and sign of the DMN coefficient is reflected in the distance between the in-DMN and out-DMN fit lines, and the magnitude of the distance coefficient by the slope of the lines. Experiment IDs: 125833030 (A), 180436360 (B). (C) Distance coefficient and (D) DMN coefficient for each of the 300 injection experiments in WT, Emx1-Cre, and Rbp4-Cre mice from the MCA. r = Pearson correlation. Experiments shown in A and B are labeled on the graphs in C and D (green and cyan borders). (E,F) Coefficients for the projections of the same 300 experiments in the lateral cortical and somatomotor masks (E) and hippocampal mask (F) as a function of the fraction of the injection inside the ICA mask for that network. The plot for the DMN coefficient from D is replicated for reference. The coefficient for 53 hippocampal experiments from the MCA is also shown for the hippocampal mask (F, light green). (G) DMN coefficients for each of the 300 WT, Emx1, and Rbp4 experiments grouped by source structure. (H) Top down cortical projection map showing the location of these experiments colored by their DMN coefficient. (I,J) The same points shown in g grouped by in-DMN and out-DMN regions (I) and module (J). (K) Cortical surface map showing the location of the 18 injection experiments in secondary motor cortex (MOs) in WT, Emx1-Cre, and Rbp4-Cre mice from the MCA, colored by the fraction of cortical projections inside the DMN mask for each experiment. The boundary of the DMN and core masks are shown in gray and cortical structure boundaries in black. (L) Coronal view of the experiments in K overlaid on a maximum intensity projection of the corresponding portion of the average template brain, colored as in K. DMN and core masks are shown in gray, experiments shown in M and N are labeled. (M,N) Cortical projection images showing two example MOs injections. Asterisks indicate the approximate injection centroid. In-DMN projections are pseudocolored cyan and out-DMN projections green. Experiment IDs: 141603190 (C), 585025284 (D). Dashed lines show the rostral-caudal position of panels O-R. (O,P) Section through the center of the injection site showing segmented injection pixels (green) overlaid on the corresponding virtual coronal section from the CCFv3 template. (Q,R) Section at the approximate rostral-caudal position with the highest projection density showing segmented projection pixels (green) overlaid on the corresponding CCFv3 virtual template section. (O-R) DMN masks shown in light gray.

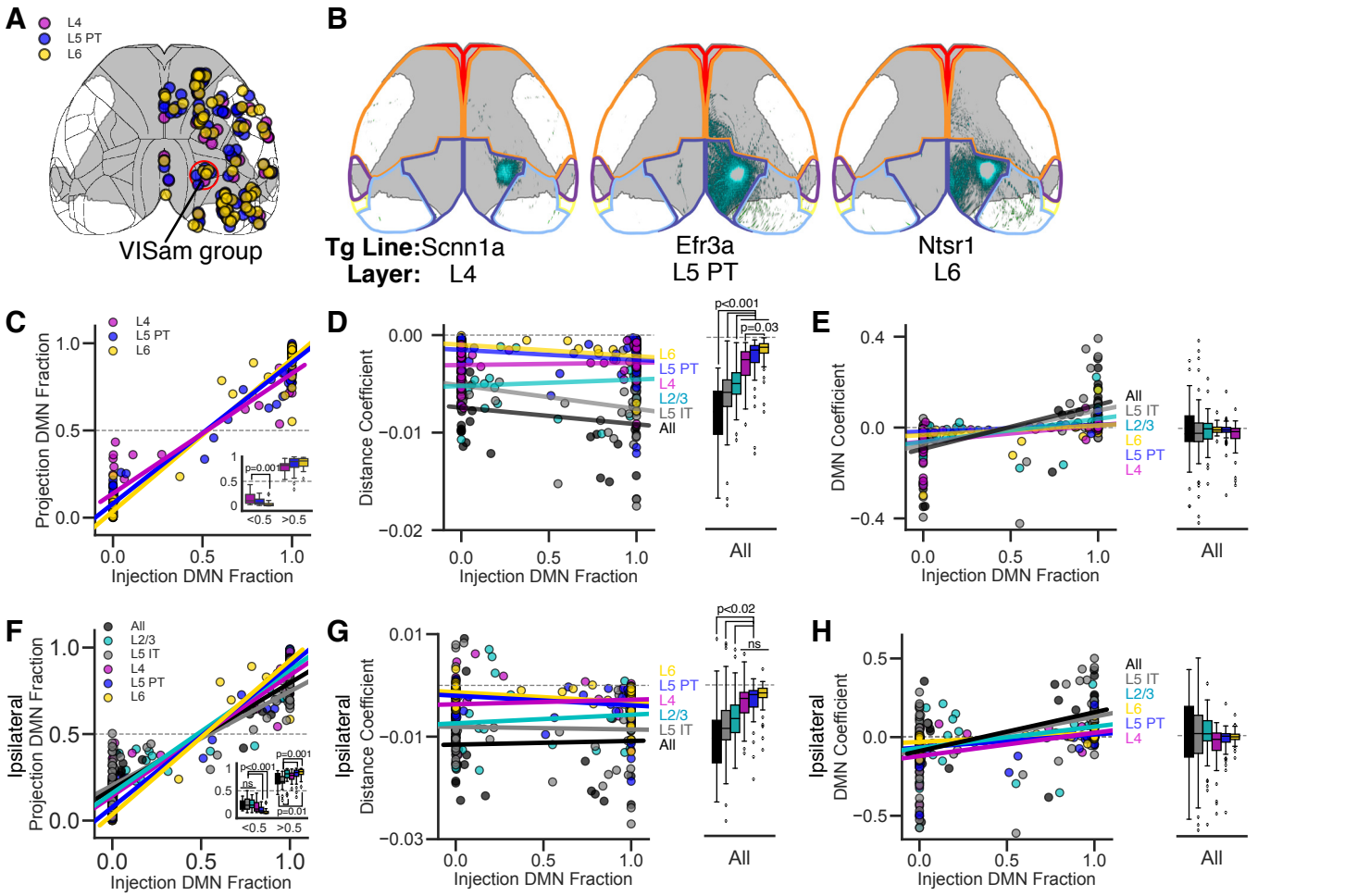

Figure S3 related to Figure 3. L4, L6, and L5 PT neurons have mainly local projections.
(A) Location of matched injection experiments in L4 selective Cre lines (magenta, n=43), L5 PT selective Cre lines (blue, n=83), and L6 selective Cre driver lines (yellow, n=61), see Methods. Red circle indicates the injection centroids belonging to the anteromedial visual cortex (VISam) group; examples shown in B. The boundary of the DMN is shown in gray and cortical structure boundaries in black. (B) Cortical projections of experiments from the VISam group in a Scnn1a mouse line selective for L4 neurons (*left*), an Efr3a mouse line selective for L5 PT neurons (*center*), and an Ntsr1 mouse line selective for L6 neurons (*right*). Experiment IDs: Scnn1a 268038969, Efr3a 309515141, Ntsr1 156671933. (C) Scatterplot and linear fit for the fraction of cortical projections inside the DMN as a function of the fraction of the injection inside the DMN for each of the 187 cortical injections shown in A. Inset shows the projection DMN fraction for injections binned by the fraction of the injection polygon inside the DMN mask. (D) Distance coefficient, and (E) DMN coefficient plotted as a function of injection DMN fraction for the set of layer-selective experiments shown in Figure 3A and panel A. Boxplots show the same points binned by the fraction of injection polygon inside the DMN mask. (F) The fraction of ipsilateral projections inside the DMN as a function of the fraction of the injection inside the DMN. Inset shows the fraction of DMN projections for injections binned by the fraction of the injection polygon inside the DMN mask. The relative values for the different layer selective Cre lines are not different from the fraction of ipsilateral and contralateral projections inside the DMN (compare with C and **Figure 3C**). (G) The relationship between the ipsilateral distance coefficient and the fraction of an injection that is inside the DMN. The relative order of the Cre lines is the same as for ipsilateral and contralateral projections (D). (H) The relationship between the DMN coefficient for ipsilateral projections and the fraction of an injection experiment that is inside the DMN. The relative order of the Cre lines is the same as for ipsilateral and contralateral projections (E).

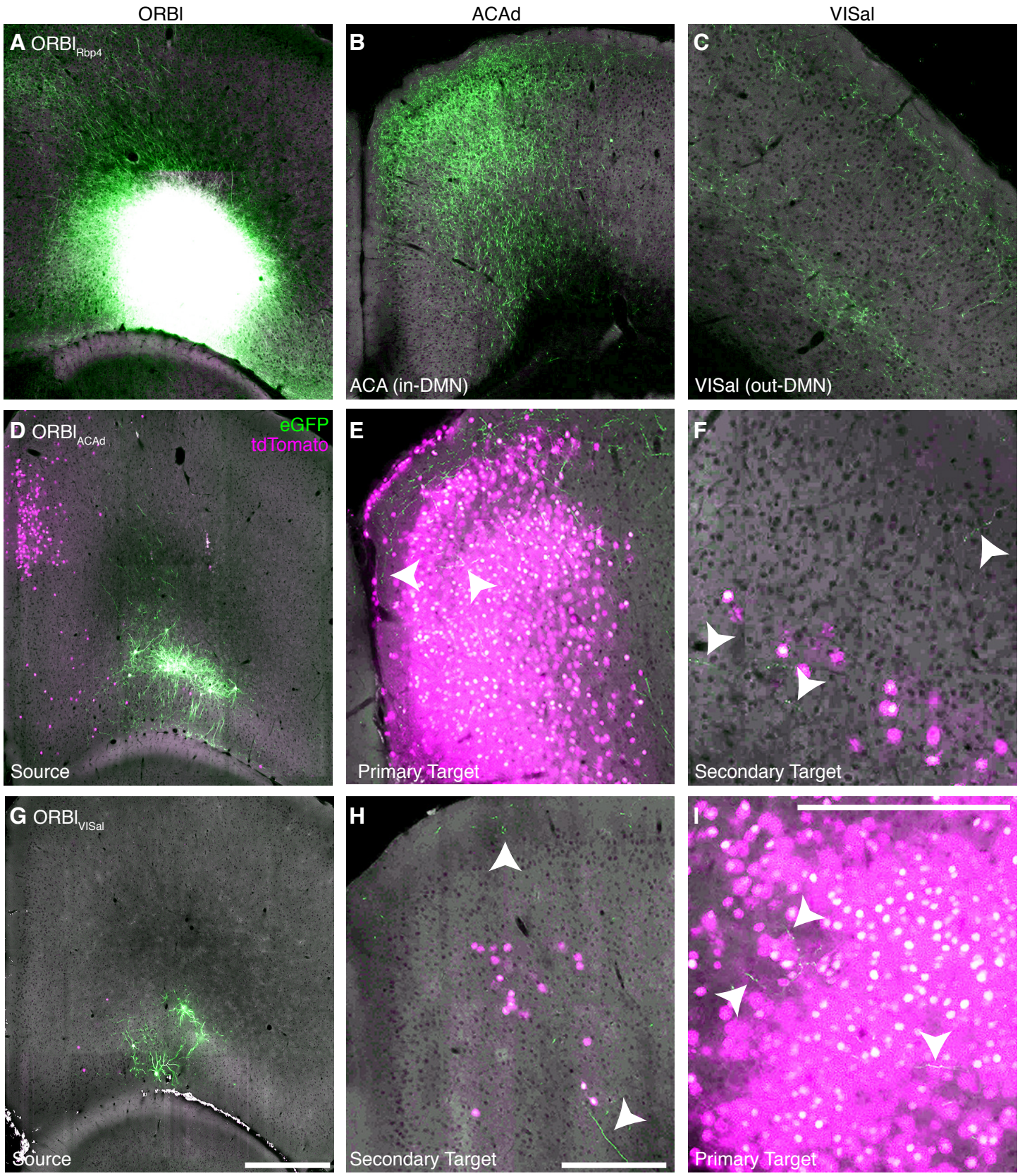

Figure S4 related to Figure 4. High magnification images of target-defined tracer experiments

(A) An ORBl injection in an Rbp4-Cre mouse. The injection site is saturated in this image so axons can be resolved. Projections from this experiment are visible in ACAd (B) and VISal (C). (D) An $ORBl_{ACAd}$ source injection (in-DMN target) showing cells coinfected with both viruses (green), and nuclei from cells infected with only CAV2-Cre (magenta). Projections from the $ORBl_{ACAd}$ cells are shown inside the CAV2-Cre injection site (E, primary target) and in VISal (F, secondary target). (G) An $ORBl_{VISal}$ source injection (out-DMN target). Projections from $ORBl_{VISal}$ cells are shown in ACAd (H, secondary target) and VISal (I, primary target). Experiment IDs: $ORBl_{Rbp4}$ 156741826, $ORBl_{ACAd}$ 571816813, $ORBl_{VISal}$ 601804603. All sections are coronal. Arrowheads point to axons. Scale=500 μm, identical for vertically-aligned images.

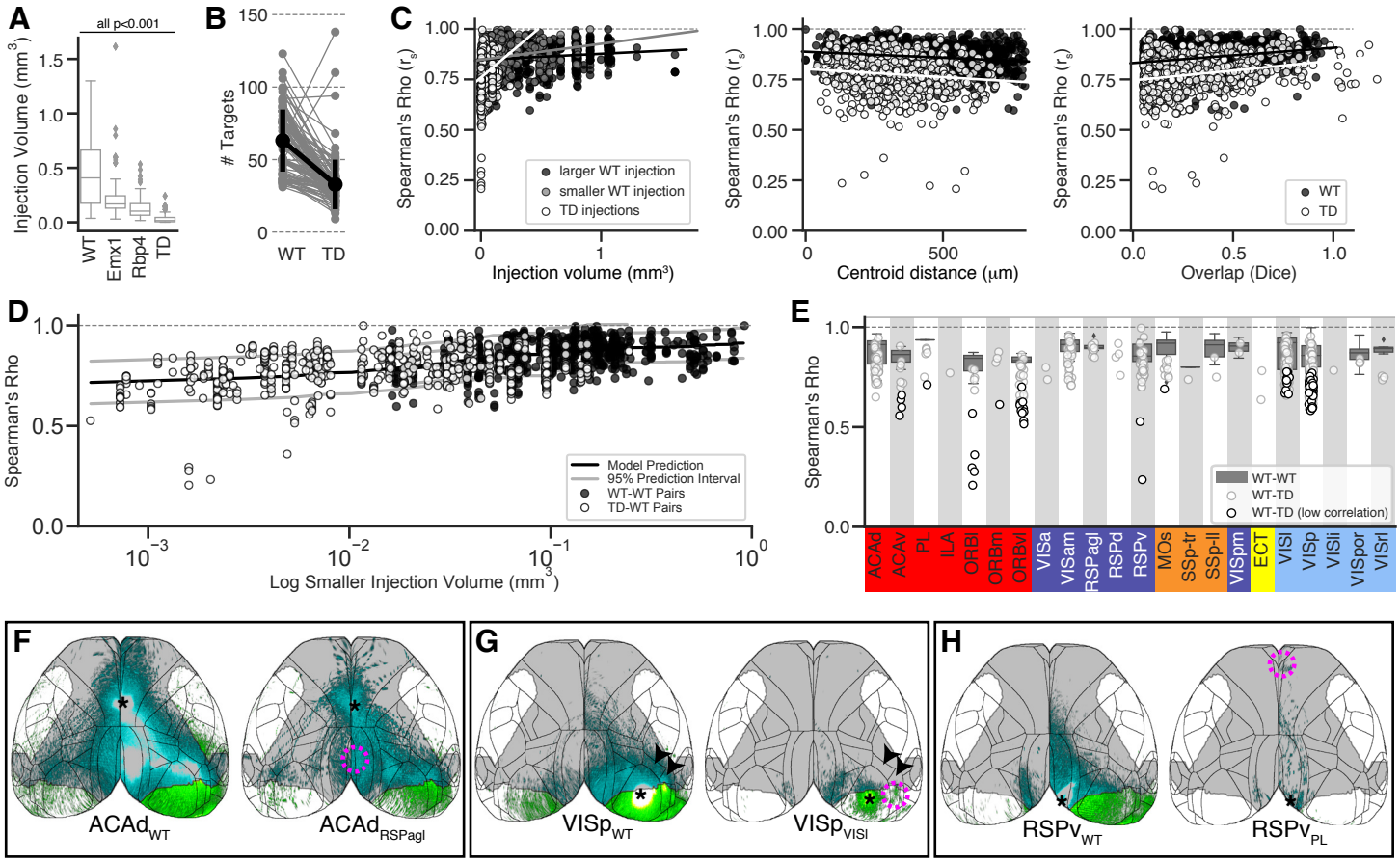

Figure S5 related to Figure 5. Quantitative characterization of target-defined experiments
(A) Injection volumes in TD experiments are significantly smaller than injection volumes in WT, Emx1-Cre, and Rbp4-Cre experiments. (B) Number of brain-wide targets with labeled axons (thresholded at log-transformed normalized projection volume > $10^{-1.5}$) in TD compared to their matched WT experiments. Thick black line: mean and standard deviation. (C) Injection volume (left), distance between injection centroids (center), and Dice overlap (right) for WT-WT experiment pairs (black and gray) and TD experiments (white). (D) Predicted (black line) and actual (points) Spearman correlation for each WT-WT (black), and WT-TD (white) injection-matched pair plotted as a function of the volume of the smaller injection in each pair. Gray lines show the 95% prediction interval. (E) Spearman's Rho (r_s) for WT – WT injection matched pairs (gray boxplots) and WT – TD injection matched pairs (white points) plotted by source. Black borders indicate "low corr" pairs (r_s below the 95% prediction interval). (F-H) Cortical projection images of matched WT (left) and TD (right) experiments with injections in ACAd (F, not low corr), VISp (G, low corr), and RSPv (H, low corr). Asterisks indicate the approximate centroid of each AAV source injection. Dashed magenta circles indicate the approximate area of the CAV2-Cre target injection. Experiment IDs: $ACAd_{WT}$ 146593590, $ACAd_{RSPagl}$ 607059419, $VISp_{WT}$ 100141219, $VISp_{VISl}$ 515920693, $RSPv_{WT}$ 112595376, $RSPv_{PL}$ 623838656. Arrowheads in the center panel show projections in VISrl and VISal in the WT experiment that are absent in the TD experiment. Additional examples of TD experiments with ACAd and VISp source injections are presented in **Figure S6**.

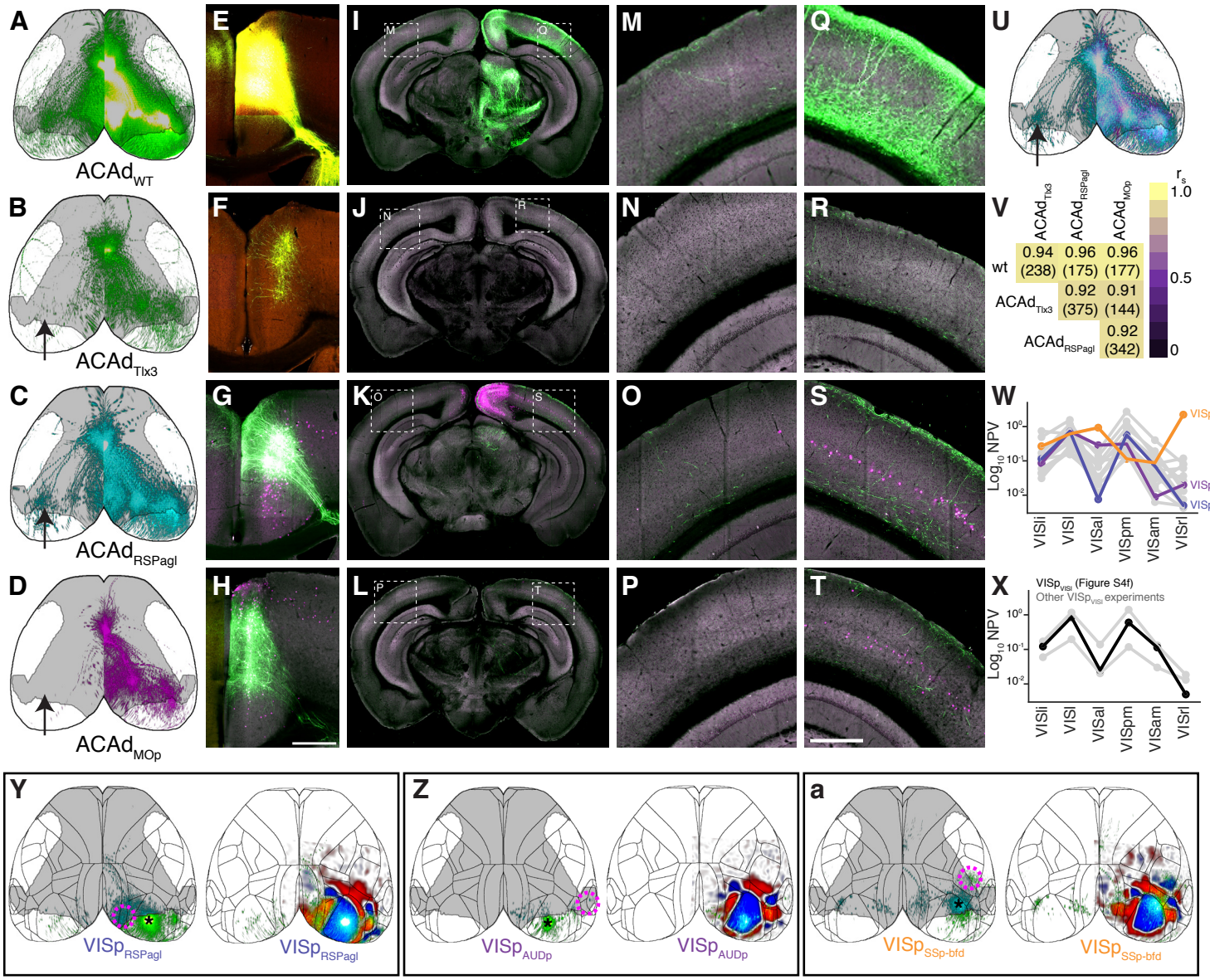

Figure S6 related to Figures 5 and S5. Additional examples of TD source injections in ACAd and VISp. (A-D) Cortical projection views for an ACAd injection in a WT mouse (A), a L5-selective Cre driver mouse (Tlx3, B), and two TD experiments (C,D). (E-H) Single section image at the approximate center of each injection site. (I-L) One coronal section from each experiment. Boxed insets show the area enlarged in (M-P, contralateral) and (Q-T, ipsilateral). (U) Overlay of the top down cortical projections from the two TD experiments in C and D. Arrows in B,C,D,U indicate the only notable difference between these experiments: contralateral projections in the $ACAd_{RSPagl}$ experiment. (V) r_s values for the four ACAd experiments shown here. Distance is given in parentheses. Scale = 500 μm. Experiment IDs: $ACAd_{WT}$ 146593590, $ACAd_{Tlx3}$ 293432575, $ACAd_{RSPagl}$ 607059419, $ACAd_{MOp}$ 475829896. (W) Normalized Projection Volume (NPV) in six visual and medial structures for three $VISp_{VISl}$ TD experiments (gray), and for the single $VISp_{VISl}$ experiment shown in Figure S4f (black). It is possible that pairing a similar VISp injection with CAV-Cre in a different VISl location would result in a different projection motif given retinotopic organization. (X) NPV in six visual and medial structures for 16 TD injections in VISp (gray). The $VISp_{RSPagl}$ projection pattern (blue) resembles the $VISp_{VISl}$ pattern in panel a, while the $VISp_{AUDp}$ (purple) projections had a different pattern with strong projections in VISli, VISl, VISal, and VISpm and no projections to VISam and VISrl. $VISp_{SSp-bfd}$ (orange) projections had yet another pattern, with projections to all the visual areas included here, and strongest in VISrl and VISal. (Y-a) Cortical projection views (left) and sign maps (right) for the $VISp_{RSPagl}$ (Y), $VISp_{AUDp}$ (Z), and $VISp_{SSp-bfd}$ (a) experiments shown in panel w. Asterisk indicates the approximate location of the AAV source injection centroid and dashed circles indicate the approximate area of the CAV2-Cre target injection. Experiment IDs: $VISp_{RSPagl}$ 501787135 , $VISp_{AUDp}$ 501837158, $VISp_{SSp-bfd}$ 539323512.The location of the injection centroid for the $VISp_{SSp-bfd}$ injection relative to the sign map shows that this source injection was located in a different part of VISp than the $VISp_{VISl}$ and $VISp_{RSPagl}$ injections, more rostral and lateral. These subtle differences in source location and their correlation to different projection patterns emphasize the importance of careful experiment matching for quantitative comparisons between TD experiments.

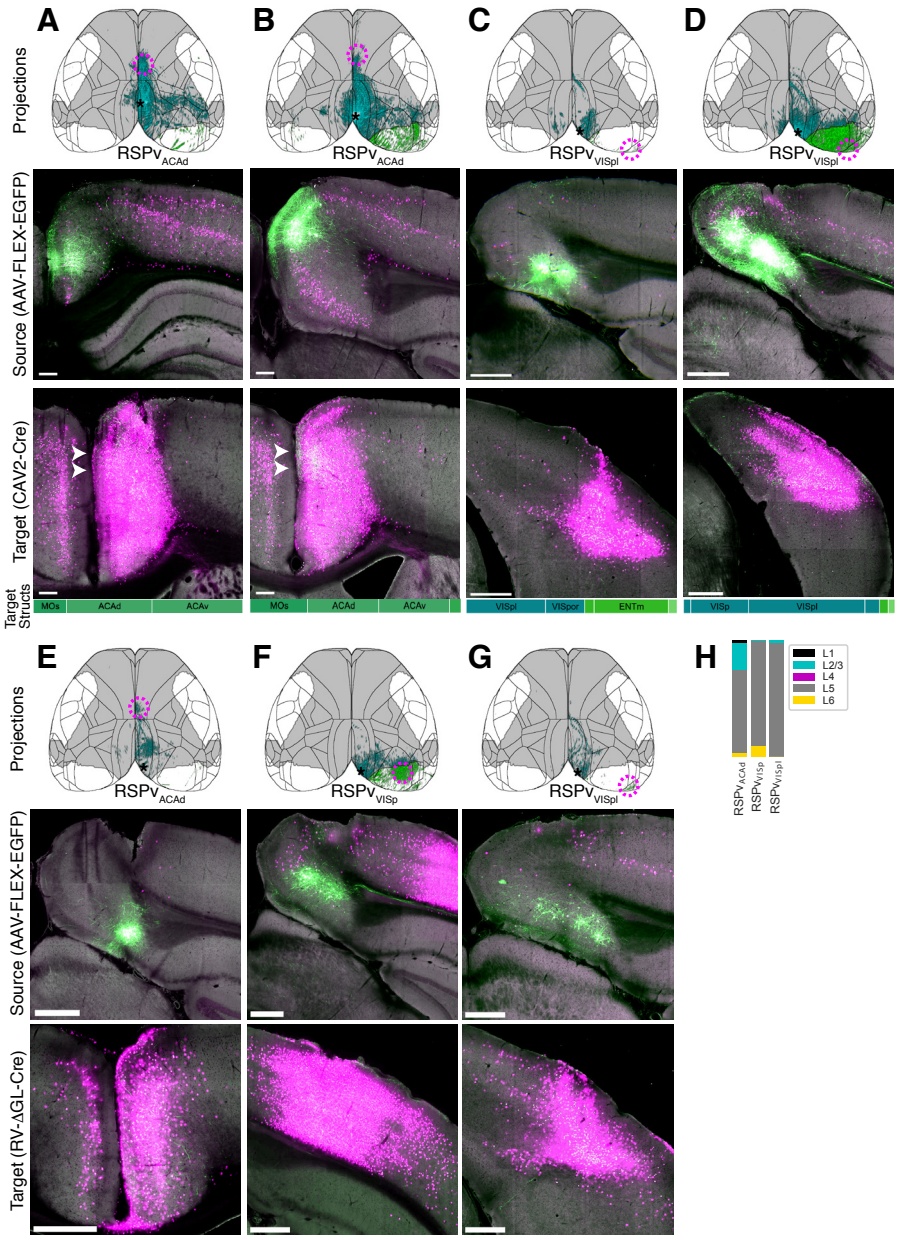

Figure S7 related to Figure 5. Midline-projecting RSPv cells are only found in caudal, ventral parts of retrosplenial cortex, and can be labeled with either CAV2-Cre or RV-ΔGL-Cre target injections. (A-D) TD experiments with CAV2-Cre virus target injections. *top*: Cortical projections. Asterisk indicates the approximate centroid of the source injection and magenta circles indicate the approximate location of the target injection. *middle*: Single image section from the approximate center of the source injection site showing the location of EGFP-expressing cell bodies for cells that were infected with both viruses. *bottom*: Single image through the approximate center of the target injection site. Bars on the bottom of the images show the regions in each CAV2-Cre injection site as the fraction of the injection polygon that overlapped with each region. (A) An RSPv$_{ACAd}$ TD injection with a source in the rostral portion of RSPv does not have a midline-projecting pattern. (B) an RSPV$_{ACAd}$ TD injection with a source in the dorsal portion of caudal RSPv does not have a midline-projecting pattern. Arrowheads in a,b point to more dense axons in ACAd than ACAv. (C) Midline-projecting RSPv cells can be labeled with a target CAV2-Cre injection in VISpl. (D) A different RSPv$_{VISpl}$ TD experiment did not label midline-projecting cells. Experiment IDs: RSPv$_{ACAd}$ (A, rostral) 475830603, RSPv$_{ACAd}$ (B, dorsal) 571647261, RSPv$_{VISpl/ENTm}$ (C) 592724077, RSPv$_{VISpl}$ (D) 666090944. (E-G) TD experiments with RV-ΔGL-Cre target injections. *top*: cortical projections. Asterisk indicates the approximate centroid of the source injection and magenta circles indicate the approximate location of the target injection. *middle*: Single image section from the approximate center of the source injection site showing the location of EGFP-expressing cell bodies for cells that were infected with both viruses. *bottom*: Single image through the approximate center of the target injection site. (E) A RSPv$_{ACAd}$ TD experiment with a midline-projecting pattern. (F) A RSPv$_{VISp}$ experiment with a visual-projecting pattern. (G) A RSPv$_{VISpl}$ experiment with a midline-projecting pattern. e-g Experimental data available through the AllenSDK. Experiment IDs: RSPv$_{ACAd}$ 605112318, RSPv$_{VISp}$ 595890081, RSPv$_{VISpl}$ 595261714. (H) Layer composition for each of the three TD source injections with RV-ΔGL-Cre as the target virus determined by registration to CCFv3. Scale = 500 μm.

Abbreviation	**Full Name**	
AAV-FLEX-EGFP	adeno-associated virus containing a flip-excision switch around the EGFP coding sequence driven by the CAG promoter	
AD	Alzheimer's disease	
BOLD	blood-oxygen-level dependent	
CAV2-Cre	canine adenovirus encoding Cre recombinase	
CCFv3	Common Coordinate Framework version 3	
CT	corticothalamic (cell type)	
DEG	differentially expressed genes	
DMN	default mode network	
Emx1	Emx1-IRES-Cre mouse line	
EPI	echo planar imaging	
FACS	fluorescence-activated cell sorting	
fMRI	functional magnetic resonance imaging	
GLM	general linear model	
ICA	independent component analysis	
ISH	In situ hybridization	
IT	intratelencephalic (cell type)	
IQR	Interquartile range	
L[#]	cortical layer (e.g. L1, L2/3, L4, L5, L6)	
MCA	(Allen) Mouse Brain Connectivity Atlas	
module	group of brain regions identified using a community detection algorithm	
network	group of interconnected neurons or brain regions	
nls-tdT	nuclear-localized td (tandem-dimer) Tomato fluorescent protein	
PT	pyramidal tract (cell type)	
r	Pearson correlation	
r_s	Spearman correlation	
Rbp4	Rbp4-Cre_KL100 mouse line	
ROI	region of interest	
rs	resting state	
RSS	residual sum of squares	
scRNA-seq	single cell RNA sequencing	
SSv4	SMART-Seq v4	
STPT	serial two photon tomography	
TD	target-defined	
WT	wild type mice	
Brain Regions		
Structure Abbreviation	**Structure Name**	**Cortical Module**
Isocortex	Isocortex	
ACAd	Anterior cingulate area, dorsal part	Prefrontal
ACAv	Anterior cingulate area, ventral part	Prefrontal
PL	Prelimbic area	Prefrontal

ILA	Infralimbic area	Prefrontal
ORBl	Orbital area, lateral part	Prefrontal
ORBm	Orbital area, medial part	Prefrontal
ORBvl	Orbital area, ventrolateral part	Prefrontal
VISa	Anterior area	Medial
VISam	Anteromedial visual area	Medial
RSPagl	Retrosplenial area, lateral agranular part	Medial
RSPd	Retrosplenial area, dorsal part	Medial
RSPv	Retrosplenial area, ventral part	Medial
SSp-tr	Primary somatosensory area, trunk	Somatomotor
SSp-ll	Primary somatosensory area, lower limb	Somatomotor
MOs	Secondary motor area	Somatomotor
SSs	Supplemental somatosensory area	Somatomotor
SSp-bfd	Primary somatosensory area, barrel field	Somatomotor
SSp-ul	Primary somatosensory area, upper limb	Somatomotor
SSp-un	Primary somatosensory area, unassigned	Somatomotor
SSp-n	Primary somatosensory area, nose	Somatomotor
SSp-m	Primary somatosensory area, mouth	Somatomotor
MOp	Primary motor area	Somatomotor
FRP	Frontal pole, cerebral cortex	Prefrontal
VISpm	posteromedial visual area	Medial
AId	Agranular insular area, dorsal part	Lateral
AIv	Agranular insular area, ventral part	Lateral
AIp	Agranular insular area, posterior part	Lateral
GU	Gustatory areas	Lateral
VISC	Visceral area	Lateral
TEa	Temporal association areas	Lateral
PERI	Perirhinal cortex	Lateral
ECT	Ectorhinal area	Lateral
VISal	Anterolateral visual area	Visual
VISl	Lateral visual area	Visual
VISp	Primary visual area	Visual
VISpl	Posterolateral visual area	Visual
VISli	Laterointermediate area	Visual
VISpor	Postrhinal area	Visual
VISrl	Rostrolateral visual area	Visual
AUDd	Dorsal auditory area	Auditory
AUDp	Primary auditory area	Auditory
AUDpo	Posterior auditory area	Auditory
AUDv	Ventral auditory area	Auditory
HPF	**Hippocampal Formation**	
CA1	Field CA1	
CA2	Field CA2	
CA3	Field CA3	
DG	Dentate gyrus	
ENTl	Entorhinal area, lateral part	
ENTm	Entorhinal area, medial part	
CTXsp	**Cortical Subplate**	
CLA	Claustrum	
OLF	**Olfactory Areas**	
AOB	Accessory olfactory bulb	
AON	Anterior olfactory nucleus	
TT	Taenia tecta	

DP	Dorsal peduncular area	
STR	**Striatum**	
CP	Caudoputamen	
ACB	Nucleus accumbens	
LSc	Lateral septal nucleus, caudal (caudodorsal) part	
TH	**Thalamus**	
LP	Lateral posterior nucleus of the thalamus	
PO	Posterior complex of the thalamus	
IAM	Interanteromedial nucleus of the thalamus	
IAD	Interanterodorsal nucleus of the thalamus	
IMD	Intermediodorsal nucleus of the thalamus	
MD	Mediodorsal nucleus of the thalamus	
RH	Rhomboid nucleus	
CM	Central medial nucleus of the thalamus	
PCN	Paracentral nucleus	
CL	Central lateral nucleus of the thalamus	
PF	Parafascicular nucleus	
MB	**Midbrain**	
SCs	Superior Colliculus, sensory-related	
PAL	**Pallidum**	

Table S1 related to Figure 1 and all text. Abbreviations.

	Structure	% of Structure in core-DMN Mask (z>1.7)	% of Structure in DMN Mask (z>1)	Fraction of projections in DMN (mean)	Fraction of projections in DMN (SD)	DMN Coefficient (mean)	DMN Coefficient (SD)	Number of Experiments
in-DMN Structures	ACAv	100	100	0.93	0.03	0.22	0.1	5
	ACAd	99	99	0.9	0.04	0.2	0.1	11
	SSp-tr	98	99	0.81	0.02	0.06	0.05	2
	ILA	97	99	0.89	0.05	0.11	0	2
	SSp-ll	97	98	0.72	0.06	0.01	0.04	6
	PL	89	89	0.81	0.04	0.12	0.09	3
	ORBvl	89	93	0.79	0.03	0.25	0.1	5
	VISa	87	96	0.77	0.03	0.08	0.02	2
	ORBm	84	88	0.78	0.03	0.19	0.06	3
	ORBl	77	93	0.67	0.12	0.05	0.15	5
	VISam	72	85	0.66	0.06	0.04	0.03	8
	RSPd	64	70	0.45	0.3	-0.04	0.03	6
	RSPv	67	78	0.69	0.19	0	0.04	11
	MOs	52	64	0.46	0.29	-0.19	0.29	18
	RSPagl	51	62	0.6	0.22	0.02	0.05	8
borderline	VISrl	42	62	0.64	0.04	0.09	0.02	6
	VISpm	32	63	0.51	0.09	-0.01	0.04	8
	AId	10	61	0.4	0.15	-0.11	0.09	3
	AIv	5	53	0.56	0	0.03	0	1
out-DMN Structures	SSp-ul	30	39	0.56	0.29	-0.07	0.07	5
	MOp	28	40	0.43	0.27	-0.19	0.23	9
	SSp-un	24	32	0.48	0	-0.01	0	1
	FRP	20	30	0.37	0	-0.17	0	1
	SSp-bfd	16	27	0.5	0.18	0	0.05	13
	VISp	6	12	0.23	0.17	-0.04	0.04	80
	SSs	0	0	0.13	0.09	-0.24	0.14	7
	SSp-n	0	0	0.09	0.03	-0.23	0.07	5
	SSp-m	0	0	0.07	0.05	-0.27	0.15	7
	Aip	0	0	0.16	0	-0.09	0	1
	GU	0	1	0.08	0.08	-0.09	0.11	2
	VISC	0	0	0.19	0.07	-0.26	0.12	4
	Tea	0	1	N/A	N/A	N/A	N/A	0
	PERI	0	0	N/A	N/A	N/A	N/A	0
	ECT	0	0	0.16	0.15	-0.04	0	2
	VISal	0	23	0.38	0.04	0	0.01	5
	VISl	0	0	0.21	0.06	-0.05	0.03	12
	VISpl	0	1	0.06	0.02	-0.06	0.07	3
	VISli	0	3	0.17	0.05	-0.08	0.02	2
	VISpor	0	0	0.12	0.04	-0.09	0.02	11
	AUDd	0	21	0.34	0.03	-0.04	0.04	2
	AUDp	0	12	0.23	0.08	-0.06	0.02	7
	AUDpo	0	26	0.28	0.13	-0.03	0.02	7
	AUDv	0	0	0.12	0	-0.1	0	1

Table S3 related to Figure 1. Cortical structures designated as in-DMN, out-DMN, and borderline for DMN membership (assigned to out-DMN). The fraction of each structure in the DMN and core masks, mean and standard deviation (SD) for the fraction of projections in the DMN for WT injection experiments in each structure, mean and SD for the DMN coefficient for WT injection experiments in each structure, and number of WT injections per structure are provided. Abbreviations in **Table S1**.